Astronomy & Astrophysics manuscript no.
(will be inserted by hand later)

arXiv:astro-ph/0102016v2 26 Apr 2001

The ATESP Radio Survey

IV. Optical Identifications and Spectroscopy in the EIS-A Region*

I. Prandoni[1,2], L. Gregorini[1,3], P. Parma[1], H.R. de Ruiter[1,4], G. Vettolani[1], A. Zanichelli[1,5], M.H. Wieringa[6], and R.D. Ekers[6]

[1] Istituto di Radioastronomia, CNR, Via Gobetti 101, I–40129, Bologna, Italy
[2] Dipartimento di Astronomia, Università di Bologna, via Ranzani 1, I–40127, Bologna, Italy
[3] Dipartimento di Fisica, Università di Bologna, Via Irnerio 46, I–40126, Bologna, Italy
[4] Osservatorio Astronomico di Bologna, Via Ranzani 1, I–40127, Bologna, Italy
[5] Istituto di Fisica Cosmica "G. Occhialini", via Bassini 15, 20133 Milano, Italy
[6] Australia Telescope National Facility, CSIRO, P.O. Box 76, Epping, NSW2121, Australia

Received 22 December 2000 / Accepted 1 February 2001

Abstract. This paper is the fourth of a series reporting the results of the ATESP radio survey, which was made at 1.4 GHz with the Australia Telescope Compact Array. The survey consists of 16 radio mosaics with $\sim 8'' \times 14''$ resolution and uniform sensitivity (1σ noise level $\sim$ 79 μJy) over the region covered by the ESO Slice Project redshift survey ($\sim$ 26 sq. degrees at $\delta \sim -40^\circ$). The ATESP survey has produced a catalogue of 2967 radio sources down to a flux limit of $\sim$ 0.5 mJy (6σ).
In this paper we present the optical identifications over a 3 sq. degr. region coinciding with the Patch A of the public ESO Imaging Survey (EIS). In this region deep photometry and 95% complete object catalogues in the I band are available down to $I \sim 22.5$. These data allowed us to identify 219 of the 386 ATESP sources present in the region. This corresponds to an identification rate of $\sim$ 57%. For a magnitude limited sample of 70 optically identified sources with $I < 19.0$ we have obtained complete and good quality spectroscopic data at the ESO 3.6 m telescope at La Silla. This data allowed us to get redshift measurements and reliable spectroscopic classification for all sources (except one).
From the analysis of the spectroscopic sample we find that the composition of the faint radio source population abruptly changes going from mJy to sub–mJy fluxes: the early type galaxies largely dominate the mJy population (60%), while star forming processes become important in the sub–mJy regime. Starburst and post-starburst galaxies go from 13% at $S \geq 1$ mJy to 39% at $S < 1$ mJy. Nevertheless, at sub–mJy fluxes, early type galaxies still constitute a significant fraction (25%) of the whole population. Furthermore we show that, due to the distribution of radio-to-optical ratios, sub–mJy samples with fainter spectroscopic follow-ups should be increasingly sensitive to the population of early type galaxies, while a larger fraction of star-forming galaxies would be expected in μJy samples. We compare our results with others obtained from studies of sub–mJy samples and we show how the existing discrepancies can be explained in terms of selection effects.

Key words. surveys – radio continuum: galaxies - galaxies:evolution

1. Introduction

Deep radio surveys have clearly indicated that normalized radio counts show a flattening below a few mJy; the first clear indications of such a flattening date back to the pioneering deep ($S_{1.4\,\mathrm{GHz}} < 1$ mJy) radio surveys undertaken in the early eighties (see Condon 1984, Kellerman et al. 1987; Windhorst et al. 1990 for reviews on radio counts available at the time), and have been confirmed by deeper and/or larger surveys (mostly at 1.4 GHz) carried out in the last decade. The counts derived from the ATESP survey, which covers an area 8 times larger than the previous surveys (Prandoni et al. 2001, paper III in this series), indicate that the upturn actually occurs at $S \lesssim 1$ mJy.

This change of slope has been interpreted as being due to the presence of a new population of radio sources (the so-called sub–mJy population) which does not show up at higher flux densities. Classical radio sources, powered by active galactic nuclei (AGN) and typically hosted by giant ellipticals and quasars are known to dominate at high flux densities (99% above 60 mJy, Windhorst et al. 1990), but their contribution steadily decreases going to fainter fluxes. At $0.1 < S_{1.4\,\mathrm{GHz}} < 1$ mJy, the median angular size of radio sources shrinks to $< 3''$

Send offprint requests to: I. Prandoni
e-mail: `prandoni@ira.bo.cnr.it`

* Based on observations collected at the European Southern Observatory, Chile, under the ESO program identifications 62.O-0883, 63.O-0467(A) and 64.O-0258(A).

and the sources are predominantly identified with blue galaxies (see e.g. Kron et al. 1985; Windhorst et al. 1985; Windhorst et al. 1990). These systems often appear disturbed, in poor groups, and/or part of merging galaxy systems. This evidence, coupled with the well-known tight far infrared/radio correlation found for many of these objects at lower redshift, as well as optical spectra with HII-like signatures similar to those of star-forming IRAS galaxies (Benn et al. 1993), suggested that the radio emission in these galaxies is the result of active star-formation ($1-100$ M$\odot$/yr).

Unfortunately, the optical identification work and subsequent spectroscopy, needed to investigate the nature of the radio sources, are both very demanding in terms of telescope time, since faint radio sources have usually very faint optical counterparts. Typically, no more than $\sim 50-60\%$ of the radio sources in sub–mJy samples have been identified on optical images. Only in the μJy survey of the Hubble Deep Field, 80% of the 111 radio sources detected have been identified (Richards et al. 1999). On the other hand, the typical fraction of spectra available is only $\sim$ 20%. Due to the long integration times needed for detection, deeper spectroscopy programmes have been undertaken only for very small sub–mJy radio samples and never went to completion. The best studied sample is the Marano Field ($\sim$ 0.3 sq. degr.), where 50% of the sources have spectra (Gruppioni et al. 1999), which allowed to determine spectral type and redshift for 29 galaxies.

When discussing results about the nature and the evolution of faint radio sources, the numbers reported above must be kept in mind. Conclusions are, in fact, limited by the low identification rate and biased by the fact that only the brightest optical counterparts have spectral information. This explains why, despite the large observational efforts, the true nature of the sub–mJy population is not yet well established. Today we know that the sub–mJy population is composed by different classes of objects (AGN, star-forming galaxies, normal elliptical and spiral galaxies), but the relative fractions are still uncertain. Gruppioni et al. (1999) found that $\sim$ 50% of the observed sources show the typical absorption spectra of early type galaxies, while late-type galaxies account for 32% of the whole population. This result is in contrast with previous ones, where a predominance of star-forming galaxies was found (e.g. in Benn et al., 47% of the sources are associated to late-type galaxies).

Recently the Phoenix survey (Hopkins et al. 1998) has given an important contribution to the knowledge of the faint radio population. Georgakakis et al. (1999) obtained spectroscopic data for 246 objects with $S_{1.4} > 0.15$ mJy and $m_R < 22.5$, corresponding to about 40% of the optically identified sample. The large numbers involved allowed the separation, on a reliable statistical basis, the mJy and sub–mJy regimes. According to their spectroscopic classification, they found that most of the emission-line sources are star-forming galaxies (contributing for $\sim$ 41% of the sub–mJy population) and that the absorption-line systems, likely to be ellipticals, dominate at flux densities > 1 mJy (46%). However absorption-line systems are also found at sub–mJy levels ($\sim$ 22%). Unfortunately a significant fraction of objects (almost 30%) could not be classified due to poor quality of the spectra, making the quoted numbers still quite uncertain.

It is therefore clear that the availability of large faint radio samples with *complete* (good quality) spectroscopy is critical in order to fully assess the nature and evolution of the mJy and sub–mJy radio sources. A significant advantage for this kind of study is obviously provided by a faint radio survey with deep photometry already available (possibly multicolor). The region we have selected fulfills these requirements at least partially. It consists of the overlap between the ATESP survey (Prandoni et al. 2000a, Paper I) and the EIS patch A photometric survey (Nonino et al. 1999).

This paper is organized as follows: in Sect. 2 we describe the ATESP-EIS sample; in Sect. 3 we define the complete sample for which we have obtained spectroscopy and we report the observations, the reduction of the spectra and the spectral classification criteria used. The ATESP-EIS sample properties are described in Sect. 4. The mJy and sub–mJy population properties as deduced from our analysis are discussed in Sect. 5. Conclusions are given in Sect. 6.

Through this paper we will use $H_0 = 100$ km s^{-1} Mpc^{-1} and $q_0 = 0.5$.

2. The ATESP–EIS Sample: Optical Identifications

Vettolani et al. (1997) made a deep redshift survey (referred to as ESP) in two strips of $22^\circ \times 1^\circ$ and $5^\circ \times 1^\circ$ at $\delta \sim -40^\circ$. They obtained photometry and spectroscopy for 3342 galaxies down to $b_J \sim 19.4$ (Vettolani et al. 1998). The same region was observed at 1.4 GHz with the Australia Telescope Compact Array. This radio survey (referred to as the ATESP radio survey) consists of 16 radio mosaics with $\sim 8'' \times 14''$ resolution and uniform sensitivity (1σ noise level $\sim$79 μJy) over the region covered by the ESP redshift survey ($\sim$ 26 sq. degrees, see details in paper I). The ATESP survey has produced a catalogue of 2967 radio sources down to a flux limit (6σ) of $\sim$ 0.5 mJy (see Prandoni et al. 2000b - paper II - and following updates at http://www.ira.bo.cnr.it/atesp).

In a 3.2 sq. degr. subregion of the $5^\circ \times 1^\circ$ strip lies the EIS (ESO Imaging Survey) Patch A, consisting of deep images in the I band out of which an object catalogue has been extracted. Further V band images are available over $\sim$ 1.5 sq. degr.. In order to identify the radio sources present in this area we used the EIS Patch A I-band *filtered* catalogue. The filtering is required to eliminate truncated objects (f.i. objects at the border of the images) and objects with a significant number of pixels affected by cosmic rays and/or other artifacts (see the discussion in Nonino et al. 1999, Sect. 5.3). This catalogue covers 3 square degrees. At I $\sim$ 22.5 the completeness of the EIS catalog is $\sim$ 95%, while it rapidly drops at fainter magnitudes. We then decided to consider in our analysis only the radio-optical associations found down to $I = 22.5$. A search circle of $3''$ radius, centered at each radio position, was chosen; this turned out to be a good compromise when inspecting Fig. 1, where the distance distribution of the radio-optical associations with $I < 22.5$ is presented. For double and triple radio sources the distance to the nearest optical counterpart is computed from the radio centroid, while for complex radio sources (e.g. sources which cannot be described by a single or multiple Gaussian fit)

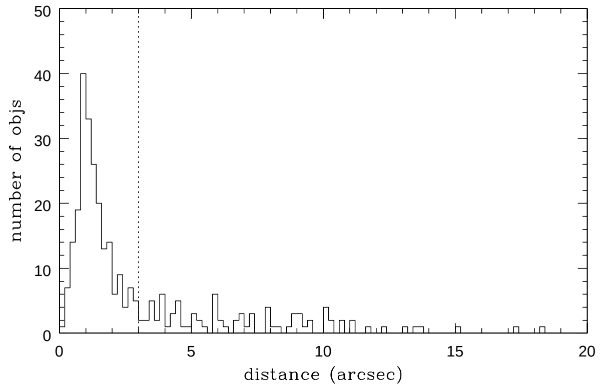

Fig. 1. Distribution of the radio-optical positional offsets between each ATESP radio source in EIS patch A and the nearest EIS object. Only radio-optical associations with $I < 22.5$ are drawn. The vertical dotted line indicates the distance cut-off ($3''$) used to define the real radio-optical identifications.

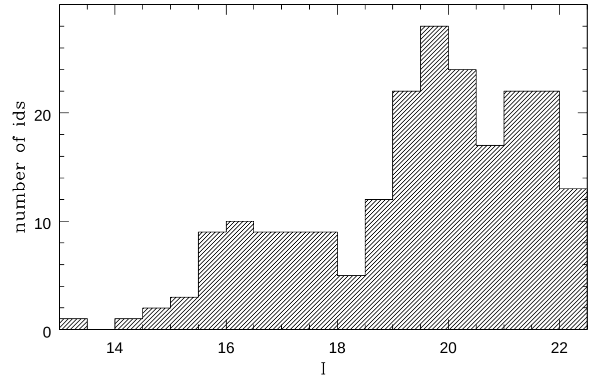

Fig. 2. I magnitude distribution for the 219 optically identified ATESP sources down to $I = 22.5$.

the distance is computed from the radio peak position. Since this position does not generally coincide with the position of the source nucleus (where the optical identification is expected to be) we allowed for distances larger than $3''$ and checked for the actual existence of optical counterpart by visual inspection of the radio-optical finding charts. As to the radio morphology, among the 386 sources three are triples (none identified), three are complex (one identified), twenty-one are doubles (six identified) and 359 are point-like (212 identified). In summary, 219 of the 386 radio sources present in this region have been identified down to I=22.5

The distribution of radio-optical pairs at distances $> 3''$ has been used to provide an estimate of the number of spurious identifications expected in the identification sample. The estimated contamination rate is $\sim 2\%$ (5/219).

Fig. 2 shows the distribution of the identified radio sources as a function of the I-band magnitude. The most interesting feature in this distribution is the strong decrease at magnitudes $I > 20$. We point out that this is not due to incompleteness effects in the optical catalogue but is a consequence of the physical radio-optical properties of our sources (see discussion in Sect. 5).

3. The ATESP-EIS Sample: Spectroscopy

From the list of 219 identified radio sources we have extracted a sample of 70 galaxies complete down to I = 19.0 and we have obtained spectra for all objects except the double radio source ATESP J224750-400143. The spectra were taken in three different runs (October 1998, September and October 1999) with EFOSC2, mounted on the ESO 3.6 meter telescope at La Silla, Chile. In the first run (October 1998) we used Grism number 11, which gives a dispersion of 2.12 Å/pixel. The scale of EFOSC2 is 0.16 arcsec per pixel, corresponding to 13.2 Å/$1''$ slit. The wavelength range covered is 3380–7540 Å. In the following runs (September and October 1999) we used Grism number 6, which gives a similar dispersion (2.06 Å/pixel, corresponding to 12.9 Å/$1''$). This grism was chosen because it is more efficient in the red part of the wavelength range covered (3860 – 8070 Å) and allows to detect the Hα line up to larger redshifts. Typical exposure times range from 15 minutes for the brightest galaxies ($I < 16.5$) to 1 hour for the faintest galaxies ($I > 18.5$). For 14 objects, spectra were already available. They had been taken with the multi-fiber spectrograph Optopus (also at the ESO 3.6 m telescope) by the ESP team (Vettolani et al. 1998). These spectra have a dispersion of 4.5 Å per pixel over the λ range 3750–6150 Å.

The reduction of the spectra was done with the IRAF package: we followed the standard procedures of bias subtraction, flat field correction, object extraction from the two-dimensional EFOSC images, sky subtraction and subsequent wavelength and flux calibration. In slightly over one half of the spectra emission lines were present (typically at least [OII] or Hα, but often other lines too); the elliptical galaxies are mostly without emission lines and the redshift is based on absorption lines like the Ca H and K lines, the G band, the Mg triplet at $\sim$ 5180 Å, and the Na D doublet. The obtained redshifts are helio-centric. The rms uncertainty in the redshifts (always determined from at least three lines) is of the order of 100 km/s, in accordance with the resolution of the spectra. The high signal-to-noise ratio of these spectra permits an unambiguous spectral classification of the whole sample. Classification of the spectral types is given in the next section.

3.1. Spectral Classification

The spectral classification criteria we used are based on visual inspection of the spectra and were followed, when necessary, by measurements of line fluxes (and/or equivalent widths) to be used in diagnostic diagrams as those presented by Baldwin et al. (1981) or Rola et al. (1997). However, the use of diagnostic diagrams is rather limited here due to the low resolution of the spectra (e.g. $H\alpha$ and [NII] lines cannot be separated) and to

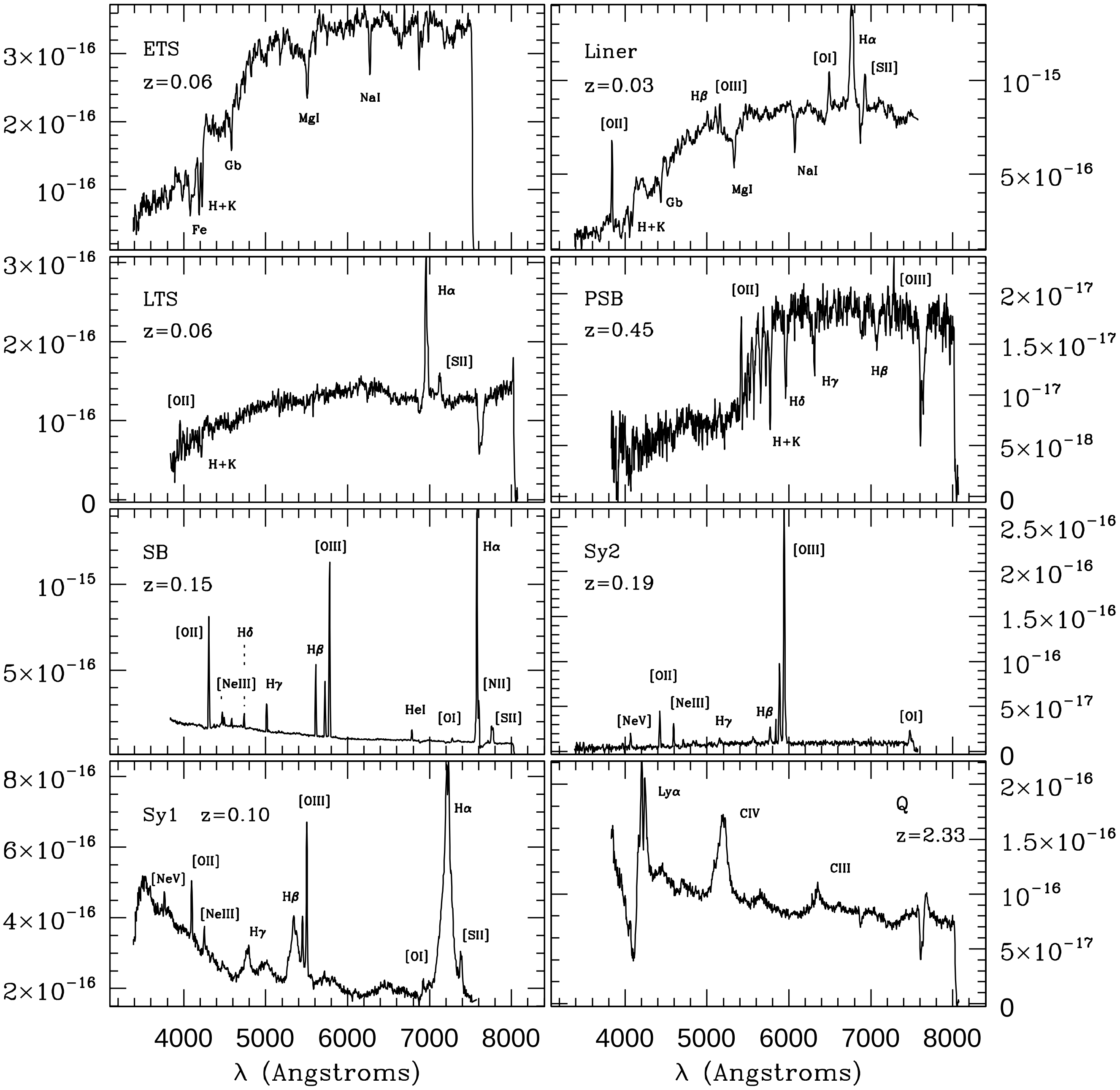

Fig. 3. Examples of the different spectral classes defined in the text. All spectra are redshifted.

the poorer signal-to-noise ratio in faint object spectra. We used the classification scheme originally proposed by Morgan and Mayall (1957) and revised by Kennicutt (1992), which is basically followed also by Georgakakis et al. (1999) and Gruppioni et al. (1999) in the study of faint radio galaxies. However, we have classified the post-starburst galaxies separately. The spectral classes we use are:

Early Type Spectrum (ETS) – Galaxies whose spectra show absorption lines coming from a mixture of late type stars characterizing ellipticals and S0s or bulge dominated spirals. The subtle difference between ellipticals and early spirals (especially an increase of the blue continuum), is not appreciable in our low resolution spectra. Faint [OII] or $H\alpha + [NII]$ emission lines may be present with equivalent width less than 3 Angstroms.

Starburst (SB) – We classify as starburst those galaxies that show spectra typical of moderate to high excitation HII regions (see McCall et al. 1985 for examples of extra-galactic HII regions) or similar to the spectrum of NGC3310 (Kennicut 1992).

Post–starburst (PSB) – We find two types of post-starburst among our galaxies spectra. a) K+A galaxies which are characterized by strong $H\delta$ absorption superposed on a typical ETS spectrum with no emission lines. Higher order Balmer absorptions are often present implying the presence of a significant

Table 1. Optical and radio properties of the complete spectroscopic sample

Name	$S_{1.4}$ (mJy)	I	V	b_j	z	Emission Lines	Spectral Class	Gr. #	Notes
ATESP J223503-394900	7.42	17.67		19.80	0.1957	[OII], [OIII]	LTS	11	
ATESP J223542-402627	0.71	16.63	18.17	18.81	0.1665		LTS	6	
ATESP J223559-393532	0.74	15.29		17.26	0.1071		ETS		ESP spectrum
ATESP J223601-393705	0.94	17.87		19.26	0.1690	[OII], [OIII], [OI], Hα, [SII]	PSB	6	Signs of SF activity
ATESP J223602-401923	2.16	15.91		18.03	0.1675	[OII], Hβ, [OIII]	PSB	11	
ATESP J223603-400420	2.96	18.57			0.5297		ETS	6	
ATESP J223606-402609	1.86	16.46	18.06	19.26	0.2053		ETS	11	
ATESP J223620-401714	17.98	18.25	20.77		0.5075		ETS	6	
ATESP J223634-402740	1.13	16.27	17.73	18.40	0.1409	[OII]	PSB		ESP spectrum
ATESP J223636-400444	0.69	16.89	18.63	19.74	0.2782		ETS	6	
ATESP J223656-402554	3.96	17.58	19.48	19.74	0.2785	[OII]	LTS	11	
ATESP J223704-393144	21.96	14.05			0.0641		ETS	11	
ATESP J223733-402141	0.70	16.96	18.25	18.99	0.1519	[OII], Hβ, [OIII]	Sy2		ESP spectrum
ATESP J223747-393612	0.76	17.63		20.14	0.2508	[OII]	LTS	6	
ATESP J223812-394018	15.12	16.58		19.10	0.2506		ETS	11	
ATESP J223845-395343	13.56	18.12			0.4541		ETS	6	
ATESP J223848-393345	0.77	15.82		17.29	0.0651	[OII], [OIII]	LTS		ESP spectrum
ATESP J223916-394125	2.05	16.94		18.95	0.1771		ETS	11	
ATESP J224011-393753	1.58	15.08		16.56	0.0645	[OII], Hβ, [OIII]	LTS		ESP spectrum
ATESP J224019-394558	3.20	18.00		21.53	0.3393	[OII], [OIII]	LTS	6	
ATESP J224106-400400	2.82	18.88	21.05		0.4662		ETS	6	
ATESP J224115-394817	1.79	14.72		16.63	0.0633	[OIII]	LTS		ESP spectrum
ATESP J224120-394844	7.95	18.91			0.5948		ETS	6	
ATESP J224139-394150	1.11	17.22		19.14	0.1961	[OII], [NeIII], Hδ, Hγ, Hβ, [OIII], [OI], Hα	Sy1	6	
ATESP J224139-394857	2.58	18.34			0.1871	[NeV], [OII], [NeIII], Hγ, Hβ, [OIII], [OI]	Sy2	11	
ATESP J224147-394855	1.93	16.89		18.73	0.1851	[OII]	LTS	11	
ATESP J224151-400634	3.33	18.69	21.27		0.5032		ETS	6	
ATESP J224157-402505	9.70	18.13	20.35	20.82	0.4265		ETS	11	
ATESP J224227-395623	28.12	18.54			0.5876		ETS	6	
ATESP J224240-400625	8.46	17.07	18.54	19.55	0.2144		ETS	11	
ATESP J224247-395539	0.60	16.15		17.84	0.0604	[OII], Hβ, Hα, [SII]	LTS	6	
ATESP J224311-393751	1.85	15.80		17.88	0.1263		PSB	11	
ATESP J224314-400255	43.17	13.42		15.23	0.0304	[OII], Hβ, [OIII], [OI], Hα, [SII]	L	11	
ATESP J224322-400839	0.72	17.61	18.63	19.33	0.2150	[OII], Hγ, Hβ, [OIII], Hα, [SII]	SB	6	
ATESP J224325-395519	0.71	18.23		20.11	0.3267	[NeV], [OII], [OIII]	LTS	6	
ATESP J224327-395904	1.15	18.65		21.34	0.2846		ETS	6	
ATESP J224342-400759	0.61	16.06	17.54	18.30	0.2164		PSB		ESP spectrum
ATESP J224417-394307	5.61	17.30		19.89	0.2832		ETS	11	
ATESP J224422-393846	0.57	17.13		18.88	0.0975	[OII], Hβ, [OIII]	SB		ESP spectrum
ATESP J224426-401916	1.93	17.40	18.84	19.58	0.2144		ETS	11	
ATESP J224448-394635	0.54	17.40			0.1549	[OII], [NeIII], Hδ, Hγ, Hβ, [OIII], HeI, [OI], Hα, [SII]	SB	6	
ATESP J224507-394702	1.24	16.60		18.46	0.1541	[OII], [OIII], [OI]	PSB	11	Signs of SF activity
ATESP J224512-395254	4.41	15.93		18.18	0.1387		ETS		ESP spectrum
ATESP J224513-400051	0.59	16.98		19.56	0.2468		ETS	6	
ATESP J224523-393440	1.19	15.21		17.38	0.0992	[NeV], [OII], [NeIII], Hγ, Hβ, [OIII], [OI], Hα, [SII]	Sy1	11	
ATESP J224547-400324	32.83	16.22		18.82	0.1937		ETS	11	Strong blue continuum
ATESP J224557-393557	2.11	16.20		16.90	0.0665	[OII], Hα, [SII]	LTS	11	
ATESP J224612-395312	0.90	18.57			0.4374	[OII]	ETS	6	
ATESP J224628-401207	1.35	15.92	17.27	18.12	0.1259		ETS	11	
ATESP J224639-393324	0.91	16.66			0.1267	[OII], Hγ, Hβ, [OIII], [OI], Hα, [SII]	SB	6	
ATESP J224640-401710	0.65	16.26	17.68	18.49	0.1488		ETS		ESP spectrum
ATESP J224654-400108	5.59	17.83			0.4011		ETS	6	
ATESP J224720-394115	19.62	17.91		20.50	0.3274	[OII]	LTS	11	
ATESP J224729-402001	0.84	16.26	17.55	18.21	0.1034	[OII], Hβ, [OIII], Hα, [SII]	PSB	6	Signs of SF activity
ATESP J224750-400143	13.31	18.68		23.15					Not observed
ATESP J224758-394046	3.78	16.25		18.16	0.1313		ETS		ESP spectrum
ATESP J224803-400513	0.67	17.41	18.00	18.04	2.3300	Lyα, CIV, CIII	Q	6	
ATESP J224811-395642	1.15	18.73		21.91	0.4539	[OII], [OIII]	PSB	6	
ATESP J224821-395707	1.91	15.71			0.1332	[OII], [NeIII], Hδ, Hγ, Hβ, [OIII], [OI], Hα, [SII]	SB	6	
ATESP J224829-394805	0.57	18.95			0.4001	[OII], Hδ, Hγ, Hβ, [OIII]	SB	6	
ATESP J224906-394246	7.41	15.84		17.96	0.1354		ETS	11	
ATESP J224911-400859	0.88	15.95	17.03	17.62	0.0646	Hα, [SII]	LTS	6	
ATESP J224913-394651	0.58	18.82			0.5457	[OII]	ETS	6	
ATESP J224941-395146	2.26	17.70		20.48	0.3282		ETS	6	
ATESP J224958-395855	1.52	17.20		19.51	0.2489		ETS	11	
ATESP J225008-400425	2.88	16.10	17.36	17.78	0.1262	[OII]	ETS		ESP spectrum
ATESP J225010-395033	0.93	17.10		18.78	0.1826	[OII], Hγ, Hβ, [OIII]	SB		ESP spectrum
ATESP J225027-394448	1.38	17.50		19.85	0.3018		ETS	11	
ATESP J225029-400332	0.75	18.81		21.48	0.5395	[OII]	LTS	6	
ATESP J225033-394646	3.16	14.72		15.23	0.0558	[OII], Hβ, [OIII]	Sy2		ESP spectrum

A star population which comes from a burst 0.1-1 Gyr old. b) Galaxies with spectra showing the simultaneous presence of Balmer absorptions and a moderate OII line (E+A galaxies, see Zabludoff et al. 1996). Other emission lines can be present. This is indicative of a somewhat younger burst or possibly highly reddened still active burst.

Late Type Spectrum (LTS) – Galaxies with spectra similar to those of late spirals (Sb, Sc, Scd, Sd) which are characterized

Table 2. Composition of the ATESP-EIS sample

Spectral Class	All		$S \geq 1$ mJy		$S < 1$ mJy	
	N	(%)	N	(%)	N	(%)
Early Type Spectrum + Liner	33	(48)	27	(60)	6	(25)
AGN	6	(9)	4	(9)	2	(8)
Late Type Spectrum	15	(22)	9	(20)	6	(25)
Starburst + post-SB	15	(22)	6	(13)	9	(39)
All	69		46	(67)	23	(33)

(with respect to ellipticals) by a) bluer stellar continuum, b) less prominent absorption lines. Emission lines are often present (typically [OII], [OIII], and/or $H\alpha+[NII]$) but only in a few cases are prominent. We notice that in a number of cases it is very difficult to assess the prominence of the bulge with respect to the disk. Such objects have been included in the LTS class. As a consequence, this class is probably contaminated by earlier-type spectra, e.g. by objects with intermediate properties between the LTS and the ETS classes.

AGN – We group here objects with evident characteristics of either Seyfert 1 (Sy1) or Seyfert 2 (Sy2) or quasar (Q) spectra.

Liner (L) – There is only one evident liner (as defined in Heckman 1980) characterized by prominent emission lines from low ionization species (e.g. [OI]).

Examples of the spectral classes are illustrated in Fig. 3. In Table 1 we present the complete spectroscopic sample: the ATESP name is listed in Col. 1; the total flux for extended radio sources or the peak flux for point-like sources is given in Col. 2. Fluxes (1.4 GHz) are corrected for systematic underestimations due to smearing and clean bias (see Paper II for details); I and V magnitudes from the EIS catalogue are given in Cols. 3 and 4, respectively; the b_j magnitude given in Col. 5, was obtained using the ROE/NRL COSMOS UKST Southern Sky Object Catalog (Yentis et al. 1992) at the web site of the US Naval Observatory; redshift is in Col. 6, prominent emission lines[1], whenever present, and the spectral class are given in Cols. 7 and 8, respectively. The last two columns report the Grism information (Col. 9) and some notes about individual spectra (Col. 10).

4. The ATESP-EIS Sample: Properties

The faint radio source composition resulting from the ATESP-EIS spectroscopic sample is presented in Table 2, where sub–mJy and mJy regimes have been considered separately. We notice that the good quality of the spectra allowed us to classify all objects. Our data clearly show that the AGN contribution does not significantly change going to fainter fluxes ($8-9$%). The same is true for late type (LTS) objects (which go from 20% to 25%). This can be due to the fact that this spectral class is probably contaminated by objects with earlier type spectra (see discussion in Sect. 3.1). More meaningful is therefore a direct comparison between the class of early type (ETS) galaxies and the starburst + post-starburst (SB + PSB) one. Early type galaxies largely dominate (60%) the mJy population, while star-formation processes become important in the sub–mJy regime: SB and post-SB galaxies go from 13% at $S \geq 1$ mJy to 39% at $S < 1$ mJy. Nevertheless, at sub–mJy fluxes, early type galaxies still constitute a significant fraction (25%) of the whole population.

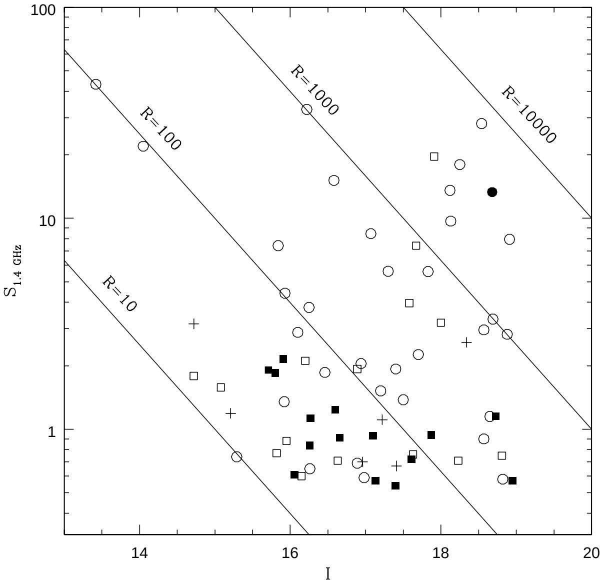

Fig. 4. 1.4 GHz flux density (in mJy) versus I magnitude; lines represent constant values of the radio to optical ratio R. Symbols represent different spectral classes: Early Type Spectrum + Liner (empty circles), Late Type Spectrum (empty squares), Starburst + post-SB (filled squares) and AGN (crosses). Also drawn is the single object for which spectroscopy is not available (filled circle).

In Fig. 4 we plot the radio flux densities against the I magnitudes for the whole sample. Superimposed are the lines representing constant values for the radio-to-optical ratios, defined following Condon (1980) as

$$R = S \cdot 10^{0.4(I-12.5)}, \tag{1}$$

where S is the 1.4 GHz flux in mJy and I is the magnitude. In Fig. 4 the sudden change in the radio source composition going from the mJy to the sub–mJy regime is immediately evident. From a closer inspection, though, it also appears that the fraction of sub–mJy sources with early type spectrum becomes more important going to fainter magnitudes. In fact at sub-mJy fluxes the number ratio of star-forming (filled squares) over early type (empty circles) galaxies is $2:1$ for $I < 18$ (8 SB/PSB galaxies against 4 ETS galaxies), while a reversed ratio is found for $I > 18$ (2 ETS against 1 SB). The latter result, even though based on a very small number of objects, may indicate that star-forming galaxies actually dominate the sub–mJy population only at bright magnitudes, as also found by Gruppioni et

---

[1] Hα is always intended as Hα+[NII].

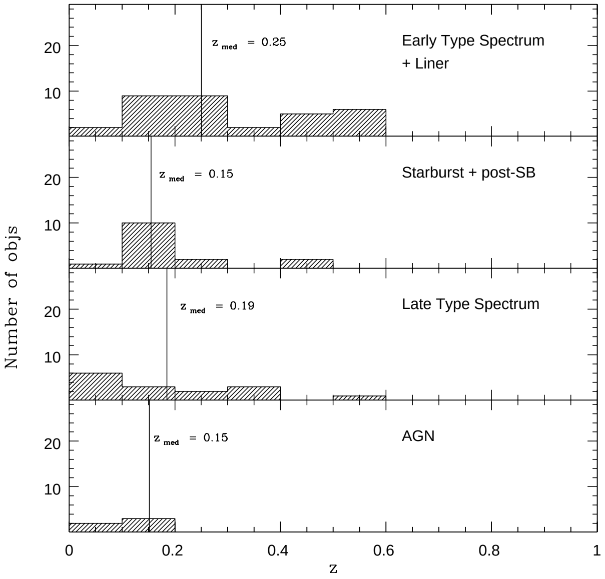

Fig. 5. Redshift distribution for the ATESP spectroscopic sample. Different spectral classes are drawn separately. From Top to Bottom: Early Type Spectrum + Liner; Starburst + Post-SB; Late Type Spectrum; AGN (the quasar at z=2.33 is not drawn and not considered in the computation of the median redshift).

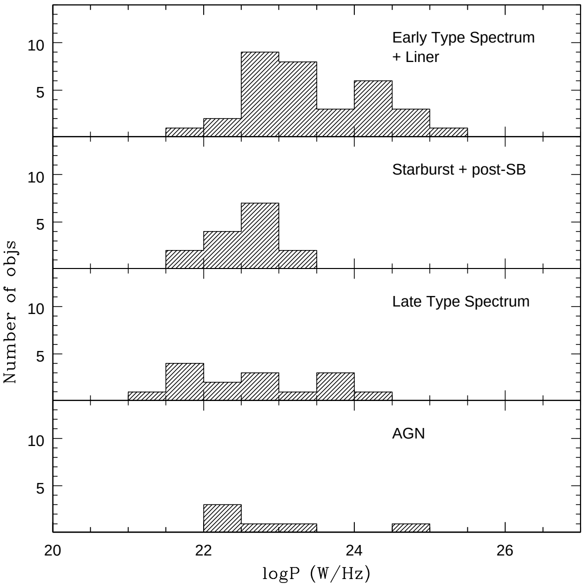

Fig. 6. Radio power distribution for the ATESP spectroscopic sample. Different spectral classes are drawn separately. From Top to Bottom: Early Type Spectrum + Liner; Starburst + Post-SB; Late Type Spectrum; AGN.

al. (1999) in the radio-optical study of the Marano Field (see discussion in Sect. 5).

The fact that star-forming galaxies dominate our sub–mJy sample only at bright magnitudes is reflected also in the redshift distribution of the different spectral classes (shown in Fig. 5). The median redshift distribution of the whole sample is z=0.20; but starburst and post-starburst galaxies are nearer than early type galaxies. Such a trend was also found in previous studies of sub–mJy (Gruppioni et al. 1999) and mJy (Magliocchetti et al. 2000) samples.

In Fig. 6 we show the radio power distribution of the different spectral classes. These distributions reflect the radio luminosity properties of the different classes. In particular, all starburst and post-starburst galaxies have powers $P < 10^{23.5}$ W/Hz, while the classes of early type objects and AGNs extend up to $P \simeq 10^{25.5}$ W/Hz. Both results are in very good agreement with the luminosity functions derived from local samples of radio sources: star-forming galaxies mostly contribute at radio powers $P < 10^{23}$ W/Hz (and become negligible in number at $P > 10^{24}$ W/Hz), while early type galaxies show a much flatter distribution in radio power, extending up to $P > 10^{26}$ W/Hz (e.g. Condon 1989). The class of late type objects cover a larger range in radio power than the class of starbursts and post-SBs, supporting the hypothesis that this class can be contaminated by earlier type objects.

Figs. 4 and 6 indicate a possible physical interpretation for the different composition found going from mJy to sub–mJy fluxes, and its possible dependence on the optical magnitude. Star-forming galaxies, characterized by weak intrinsic radio emission, have low radio-to-optical ratios (typically $10 < R < 100$, see Fig. 4), while early type galaxies cover a much larger range in radio power, and hence in R, becoming the dominant population at $R > 100$. If this behaviour holds going to fainter fluxes and magnitudes, sub–mJy samples with fainter spectroscopic follow-ups should be increasingly sensitive to the population of early type galaxies, while, at a given optical limit, a larger fraction of star-forming galaxies would be expected in μJy samples, as supported by the study of the μJy sources in the Hubble Deep Field, the majority of which seem to be associated with star-forming galaxies (Richards et al. 1999).

This hypothesis is also supported by Fig. 7, where we present the distribution in R for both the sample of all the radio sources identified down to $I = 22.5$ (empty histogram) and the 70 objects of the spectroscopic sample ($I < 19.0$) (shaded histogram). In fact the spectroscopic sample essentially exhausts the objects with low radio-to-optical ratio, while the optically fainter objects mostly have $R >> 100$. This indicates, even accounting for some evolution, that they are essentially early type galaxies or AGN's. Deeper spectroscopy for the ATESP-EIS sample will be crucial in order to verify this indication on a reliable statistical basis and to quantify the importance of evolutionary effects in the faint radio population.

As a final remark we notice that the position of the only object with no spectroscopy available in the flux-magnitude diagram (filled circle at $R \sim 4000$), together with a double-component radio morphology, points toward a nuclear origin for its radio emission.

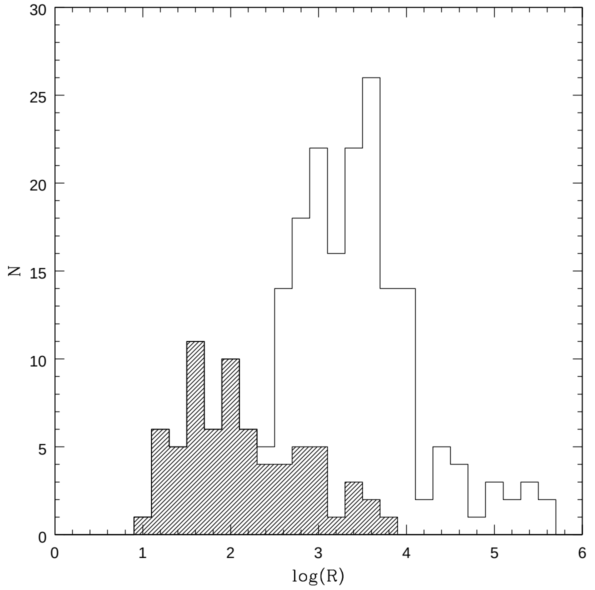

Fig. 7. Distribution of the radio-to-optical ratio R for the 219 identified galaxies down to $I = 22.5$ (empty histogram) and for the 70 galaxies with $I < 19.0$ of the spectroscopic sample (shaded histogram).

5. The mJy and sub–mJy Population

As already discussed in Sect. 1, the results obtained from the study of faint radio samples are not completely in agreement with each other and therefore the nature of the mJy and sub–mJy radio population is not yet conclusively established. This is due to both the limited size of the faintest radio surveys and to the limited optical follow-up available.

The possibility that selection effects could play an important role in this kind of study, was first recognized by Gruppioni et al. (1999) from the study of the Marano Field. They found a higher fraction of early type galaxies than in previous studies: 50% of the sources identified have colours and spectral features typical of early type galaxies, against e.g., the 9% found by Benn et al. (1993). According to the authors, this discrepancy can very likely be ascribed to the deeper optical magnitude limit reached in the Marano Field, since the fraction of sources identified with early type galaxies abruptly increases at magnitudes $B > 22$, which is approximately the limit of the sample studied by Benn et al. (1993).

In order to properly compare the results reported in the literature, it is therefore very important to take into account the differences in limiting flux and magnitude of the available radio samples.

If we assume (as suggested in Sect. 4) that a radio-to-optical ratio $R \simeq 100$ separates the locus where the star-forming population dominates ($R < 100$) from the one dominated by the early-type population ($R > 100$), we can set a limit on the brightest limiting magnitude required in the spectroscopy follow-up, in order to make the radio-optical sub–mJy studies increasingly sensitive to the early-type population. Inverting Eq. (1), we find

$$I_{100} > 17.5 - 2.5 \log S \qquad (2)$$

where I_{100} is defined as the magnitude limit corresponding to $R > 100$ and depends on the radio flux S.

In Table 3 (Column 3) we report the different values of I_{100} computed assuming $S = S_{lim}$ (S_{lim} is given in Column 2) of the most recent 1.4 GHz mJy and sub–mJy samples with radio-optical studies available. The samples are sorted on increasing values of the quantity $I_{lim} - I_{100}$ (ΔI in Column 5), where I_{lim} is the limiting magnitude of spectroscopic follow-up in each sample. To make the comparison among the different samples easier we translated all the limiting magnitudes to I-band values, assuming indicatively $R - I = 0.5$ and $B - I = 1.5$. In the following columns we give the relative fractions for the different classes of objects found in each sample. To allow for the many sub-classes defined by different authors we grouped the objects in three main classes: Early Type galaxies (E), Late Type galaxies (L) and Active Galactic Nuclei (AGN). The Late Type class contains starburst, post-starburst and normal spirals. The fourth class (O) contains any other kind of object which cannot be included in the first three classes. Besides a number of objects classified as stars, they are mostly unclassified objects due to failed and/or poor quality spectra.

Under the hypothesis that the important issue in determining the composition of the faint radio population it is neither the radio flux nor the optical magnitude, but a combination of the two quantities, the relative importance of early type objects should increase with increasing ΔI, that is going through the table, from the B93 sample (the one studied by Benn. et al. 1993) to the Marano Field (MF, Gruppioni et al. 1999). Even if the differences among the quoted fractions in the different samples are not statistically relevant due to the poor number of objects involved, it is interesting to note that this trend is confirmed for both the mJy and the sub–mJy sample. The only exception is represented by the Phoenix Deep Field (PDF, Georgakakis et al. 1999), where a fraction of early type objects smaller than expected is found. It is worth noticing though that the high percentage of unclassified objects makes the PDF result quite uncertain. This uncertainty is probably more severe for the class of the early type galaxies. In fact most of the failed and/or poor quality spectra correspond to objects with very faint magnitudes, where many early type objects are expected. Another bias against early type objects is the fact that pure absorption spectra (typical of early type galaxies) are more difficult to obtain than emission line spectra (typical of late type objects and AGNs). The same uncertainty affects the numbers reported for the Benn et al. sample, where the quoted fractions have to be considered as lower limits. With this caveat, the expected trend for a decreasing fraction of Late-type objects at sub–mJy fluxes with increasing ΔI is verified.

Very interesting is the fact that the fraction of AGNs is very similar (10-15%) in all the samples and in both flux regimes. This class is also probably the least affected by uncertainties due to poor spectroscopy, because in general AGNs show very strong emission lines. Since these faint radio surveys are mostly sensitive to small radio-to-optical ratios ($R < 1000$), this result

Table 3. Comparison with other 1.4 GHz mJy and sub–mJy samples

Survey	S_{lim} (mJy)	I_{100}	I_{lim}	ΔI	$S \geq 1$ mJy E (%)	L (%)	AGN (%)	O (%)	N_{tot}	$S < 1$ mJy E (%)	L (%)	AGN (%)	O (%)	N_{tot}
B93	0.1	20.0	20.5	0.5	33	22	11	33	18	3	54	13	30	69
FIRST	1.0	17.5	18.1	0.6	52	24	15	9	46	-	-	-	-	-
ATESP-EIS	0.5	18.3	19.0	0.7	60	33	9	-	46	25	65	8	-	23
PDF	0.2	19.3	21.0	1.7	46	11	11	31	71	22	41	13	25	175
MF	0.2	19.3	23.0	3.7	73	9	18	-	11	39	43	13	4	23

B93: Benn et al. 1993 FIRST: Magliocchetti et al. 2000 ATESP-EIS: this paper PDF: Georgakakis et al. 1999
MF: Gruppioni et al. 1999

can give a reliable constraint on the number density of low luminosity AGNs.

With this kind of arguments it is also possible to explain the general trend for higher fractions of early type objects at mJy fluxes than at sub–mJy fluxes: at $S \geq 1$ mJy the $R < 100$ population is expected at very bright magnitudes ($I < I_{100} \leq 17.5$), where the existing samples (covering areas from a fraction of a sq. degr. to a few sq. degr.) are severely volume limited.

This analysis seems to be able to reconcile, at least qualitatively, the discrepancies found in the literature about the nature of the faint radio sources. In particular it is very promising that in the two samples where the change of the population with the optical magnitude has been investigated (the ATESP-EIS and the MF) the computed values for I_{100} corresponds very well to the magnitude where the change has been found. In the ATESP-EIS we found an increase of early type objects at $I > 18$ (to be compared with $I_{100} = 18.3$), while in the MF the same increase is found at $R > 20$ (see Fig. 4(b) in Gruppioni et al. 1999), roughly corresponding to $I > 19.5$ (to be compared with $I_{100} = 19.3$).

As a final remark we notice that the strong decrease at faint magnitudes in the distribution of identified radio sources as a function of I magnitude shown in Fig. 2 can be explained, when we consider that at $I > 20$ the ATESP-EIS sample is sensitive only to radio sources with $R > 500 - 1000$ at fluxes of the order of $0.5 - 1$ mJy. Such values correspond to early type galaxies and/or AGNs, which are not the dominant population in optically selected samples like the EIS. A similar result was found by Georgakakis et al. (1999) in the PDF sample, where the proportion of star-forming galaxies was found to decrease relative to those of early type systems and AGNs at magnitudes $R > 19.5$. On the other hand, the authors could not draw firm conclusions from this result due to selection effects and incompleteness severely affecting their sample at these magnitudes. From our analysis we can argue that the decrement of star-forming galaxies found in the PDF sample at $R > 19.5$ is probably mostly real, since we expect this sample to become increasingly insensitive to star-forming galaxies at magnitudes $I > I_{100} = 19.3$ (or $R > 19.8$).

6. Conclusions

We have studied the radio-optical properties of a magnitude limited sample of 70 radio sources with spectroscopy available ($I < 19.0$). From our analysis we find that the composition of the faint radio sources abruptly changes going from mJy to sub–mJy fluxes: the early type galaxies largely dominate the mJy population (60%), while star forming processes become important in the sub–mJy regime. Starburst and post-starburst galaxies go from 13% at $S \geq 1$ mJy to 39% at $S < 1$ mJy. Nevertheless, at sub–mJy fluxes, early type galaxies still constitute a significant fraction (25%) of the whole population.

We argue that the relative fractions found for the two classes of star-forming and early type galaxies mainly depend on the fact that star-forming galaxies dominate at low radio-to-optical ratios ($R < 100$), while early type objects dominate at $R > 100$. Under this hypothesis it is possible to reconcile the discrepancies found from the radio-optical analysis of different sub–mJy radio samples, by taking into account the differences in limiting radio flux and optical magnitude.

If this behaviour holds going to μJy fluxes and to fainter magnitudes than reached by current studies, we expect that faint radio samples with fainter spectroscopic follow-ups will be increasingly sensitive to the population of early type galaxies, with a larger fraction of star-forming galaxies in μJy samples (given the same optical limiting magnitude). In particular, for a given radio sample, it would be possible to estimate a critical value for the optical magnitude, corresponding to the transition from star-forming to early type galaxy population: at brighter magnitudes the dominant class would be the one of star-forming galaxies, while at fainter magnitudes the early type galaxies would become the main class. This would also correspond to a limit in redshift for the star-forming class that populate a given faint radio sample. In other words, studies based on the star-forming portion of sub–mJy samples (like f.i. the analysis of the evolution of the star formation rate with the cosmic time) can give information up to limited redshifts ($z < 0.5$), while larger redshift values (up to $z \sim 1$) can be probed only by μJy samples.

In order to verify this hypothesis and check whether evolutionary effects could play an important role in changing this scenario, complete optical follow-ups down to very faint magnitudes ($I > 25$) for statistically relevant faint radio samples are needed. To avoid bias and/or incompleteness effects at the faintest magnitudes it is also very important to obtain good quality spectroscopy.

Acknowledgements. EIS observations have been carried out using the ESO New Technology Telescope (NTT) at the La Silla observatory under Program-ID Nos. 59.A-9005(A) and 60.A-9005(A). I.P. thanks the ESO staff and all the people directly and indirectly involved in the EIS Imaging Survey for their hospitality and support, during the period spent in Garching as a member of the EIS team.
The spectroscopy data were taken at the 3.6 m telescope at ESO La Silla Observatory under the ESO program identifications 62.O-0883, 63.O-0467(A) and 64.O-0258(A). We thank the ESP team, and in particular Elena Zucca and Roberto Merighi, for providing detailed information about the ESP spectra used in this work. Roberto Fanti is acknowledged for many useful comments. We are grateful to the anonymous referee for a number of useful suggestions.
The authors acknowledge the Italian Ministry for University and Scientific Research (MURST) for partial financial support (grant COFIN 99-02-37).

References

Baldwin J.A., Phillips M.M., Terlevich R. 1981, PASP, 93, 5
Benn C.R., Rowan-Robinson M., McMahon R.G., Broadhurst T.J., Lawrence A. 1993, MNRAS, 263, 98
Condon J.J. 1980, ApJ, 242, 894
Condon J.J. 1984, ApJ, 287, 461
Condon J.J. 1989, ApJ, 338, 13
Georgakakis A., Mobasher B., Cram L., et al. 1999, MNRAS, 306, 708
Gruppioni C., Mignoli M., Zamorani G. 1999, MNRAS, 304, 199
Heckman T., 1980, A&A 87, 152
Hopkins A.M., Mobasher B., Cram L., Rowan-Robinson M. 1998, MNRAS, 296, 839
Kennicut, R.C., 1992, ApJ 388, 310
Kellerman K.I. & Wall J.V. 1987, in “Observational Cosmology”, IAU Symp. 124, eds. Hewitt et al., p. 545
Kron R.G., Koo D.C., Windhorst R.A. 1985, A&A, 146, 38
McCall M.L., Rybski P.M., Shields, G. A. 1985, ApjS, 57, 1
Magliocchetti M, Maddox S.J., Wall J.V., et al. 2000, MNRAS, 318, 1047
Morgan W.W., Mayall N.U. 1957, PASP, 69, 291
Nonino M., Bertin E., da Costa L., et al. 1999, A&AS, 137, 51
Prandoni I., Gregorini L., Parma P., et al., 2000a, A&AS 146, 31 (Paper I)
Prandoni I., Gregorini L., Parma P., et al., 2000b, A&AS 146, 41 (Paper II)
Prandoni I., Gregorini L., Parma P., et al. 2001, A&A 365, 392 (Paper III)
Richards E.A., Fomalont E.B., Kellermann K.I., et al. 1999, ApJ, 526, L73
Rola C.S., Terlevich E., Terlevich R.J. 1997, MNRAS, 289, 419
Rowan-Robinson M., Benn C.R., Lawrence A., McMahon R.G., Broadhurst T.J. 1993, MNRAS, 263, 123
Vettolani G., Zucca E., Merighi R., et al. 1998, A&AS, 130, 323
Windhorst R.A., Miley G.K., Owen F.N., Kron R.G., Koo D.C. 1985, ApJ, 289, 494
Windhorst R.A., Mathis D., Neuschaefer L. 1990, in Evolution of the Universe of Galaxies, ed. R.G. Kron, p. 389
Yentis,D.J., Cruddace R.G., Gursky H., et al. 1992, in “Digitized Optical Sky Surveys”, eds. MacGillivray H.T. & Thomson E.B., p. 67
Zabludoff A.I., Zaritsky D., Lin H. et al. 1996, ApJ, 466, 104